A Letters Journal Exploring
the Frontiers of Physics

OFFPRINT

Disorder-induced mobility edges and heat flow control in anharmonic acoustic chains

M.V. Ivanchenko and S. Flach

EPL, **94** (2011) 46004

A Letters Journal Exploring the Frontiers of Physics

May 2011

EPL, **94** (2011) 46004
doi: 10.1209/0295-5075/94/46004

www.epljournal.org

Disorder-induced mobility edges and heat flow control in anharmonic acoustic chains

M. V. Ivanchenko[1,2(a)] and S. Flach[2]

[1] *Theory of Oscillations Department, University of Nizhniy Novgorod - Nizhniy Novgorod, Russia*
[2] *Max-Planck-Institut für Physik komplexer Systeme - Nöthnitzer Str. 38, 01187 Dresden, Germany, EU*

received 24 December 2010; accepted in final form 11 April 2011
published online 10 May 2011

PACS 63.20.Pw – Localized modes
PACS 63.20.Ry – Anharmonic lattice modes
PACS 05.45.-a – Nonlinear dynamics and chaos

Abstract – We control the thermal conductivity of anharmonic acoustic chains by varying the strength of disorder in the interaction. It induces mobility edges in the phonon spectrum. Therefore we limit the amount of extended modes which can ballistically propagate. The rest of the modes becomes localized and opens a diffusive heat conductivity channel. The localized modes are sensitively controlling the contact resistances at the edges. Analytical arguments and numerical results yield several crossovers between dominating heat channels, when varying the system size and the temperature.

Low-dimensional systems can show deviations from the Fourier law, resulting in anomalous heat conductivity. These effects have recently become a matter of experimental and applied interest in the context of nanotube systems. These issues even inspired research on solid-state thermal rectifiers and nanotube phonon waveguides [1]. An anomalous dependence of the thermal conductivity $\mathcal{K}$ on the nanotube length N was observed in pioneering experiments with carbon and boron-nitrid nanotubes, yielding $\mathcal{K} \propto N^{\alpha}$, $\alpha \sim 0.5$–0.6 [2]. Similar scaling laws are expected in nanowires [3]. In both cases phonons were reported to be the main heat flux carriers. Spatial disorder and anharmonic potential terms are the main sources of phonon scattering in these systems. Simulations with realistic models also indicate that disorder [4] and anharmonicity [5] generate anomalous thermal conductivity.

One-dimensional momentum-conserving arrays serve as simple models to study anomalous thermal conduction [6]. Despite intense research, a quantitative understanding of the main characteristics of anomalous conductivity is still lacking [7–9]. Mostly harmonic chains with disorder, or anharmonic ordered chains were studied. However, harmonic systems do not equilibrate and the conductivity depends on the boundary conditions and the spectrum of the thermal noise. On the other hand, for anharmonic ordered systems one lacks control over the number of relevant long wavelength modes which are assumed to contribute to anomalous conductivity. The interplay between disorder and anharmonicity was touched in refs. [10,11], where the regime of normal conductivity [10] was questioned due to finite-size effects [11]. Still, *e.g.*, the contribution of the heat transfer through localized modes was not addressed. Also the experimentally measured exponent α [2] is larger than the predicted one [11].

In this letter we uncover and study the intricate impact of the disorder-induced mobility edge on the thermal conductivity of the Fermi-Pasta-Ulam (FPU) chain with fixed boundaries. Upon variation of the temperature and the chain size we observe transitions between the following regimes: i) insulating behavior with $\alpha < 0$, ii) normal-like conductivity, $\alpha \sim 0$, iii) disorder-driven anomalous conductivity, $\alpha \sim 0.52$–0.58, iv) nonlinearity-driven anomalous conductivity, $\alpha \sim 0.38$. The crossovers and the scaling of $\mathcal{K}$ are explained by analyzing the properties and interaction of localized and delocalized modes, which are continued into the nonlinear regime, and by emerging new heat conductivity channels. We show that *anharmonic disordered* systems offer a better way to study the mechanisms of anomalous conductivity, being also more realistic models for experimental setups.

We consider the FPU-β chain of N equal masses, with disorder in the harmonic spring constants, and additional

(a) E-mail: ivanchenko@rf.unn.ru

quartic anharmonicities in the spring potential

$$H = \frac{1}{2}\sum_{n=1}^{N} p_n^2 + \sum_{n=1}^{N+1}\left[\frac{1}{2}(1+D\kappa_n)(x_n - x_{n-1})^2 + \frac{\beta}{4}(x_n - x_{n-1})^4\right], \quad (1)$$

where $x_n(t)$ is the displacement of the n-th particle from equilibrium, $p_n(t)$ its momentum, $\kappa_n \in [-1/2, 1/2]$ are random, uniform, and uncorrelated, $\langle \kappa_n \kappa_m \rangle = \sigma_\kappa^2 \delta_{n,m}$. We apply fixed boundary conditions $x_0 = x_{N+1} = 0$.

The heat conductivity is measured using a standard approach, when thermal baths are attached to the chain ends and generate a temperature gradient and heat current along the chain [7]. We implement Nosé-Hoover thermostats by adding the terms $-\zeta_\pm \dot{x}_{1,N}$ to the respective equations of motion, where $\dot{\zeta}_\pm = \dot{x}_{1,N}^2/T_\pm - 1$. The heat flux along the chain is defined as the time average of $j = -\frac{1}{2}\sum_n (\dot{x}_{n+1} + \dot{x}_n)[(1+D\kappa_{n+1})(x_{n+1} - x_n) + \beta(x_{n+1} - x_n)^3]$ [7]. The heat conductivity coefficient $\mathcal{K} = jN/(T_+ - T_-)$. We use the mean temperature $T = (T_+ + T_-)/2$ as a control parameter corresponding to the energy density $\langle E_n \rangle = k_B T = T$. We set $k_B = 1$ and $(T_+ - T_-)/T = 0.5$.

We start with the canonical transformation from the normal modes of the harmonic lattice in the absence of disorder: $x_n(t) = \sum_{q=1}^{N} Q_q(t) z_{qn}$ which defines the mode space with N coordinates $Q_q(t)$ and eigenvectors $z_{qn} = \sqrt{\frac{2}{N+1}} \sin\left(\frac{\pi q n}{N+1}\right)$. Here $q = 1, \ldots, N$ denotes the mode number. In the presence of anharmonicity and disorder the equations of motion in normal mode space are modified:

$$\ddot{Q}_q + \omega_q^2 Q_q = -\nu \sum_{p,r,s=1}^{N} C_{q,p,r,s}\omega_q\omega_p\omega_r\omega_s Q_p Q_r Q_s - d\sum_{p=1}^{N} \omega_q \omega_p K_{q,p} Q_p. \quad (2)$$

Here $\omega_q = 2\sin\frac{\pi q}{2(N+1)}$ are the normal mode frequencies. The coupling coefficients $C_{q,p,r,s}$ [12] control the selective anharmonic interaction between modes, and the coefficients $K_{q,p} = \frac{2}{N+1}\sum_{n=1}^{N} \kappa_n \cos\frac{\pi q(n-1)/2}{N+1} \cos\frac{\pi p(n-1)/2}{N+1}$ [13] describe the mode interaction due to disorder. The nonlinearity and disorder parameters $\nu = \beta/(N+1)$, $d = D/\sqrt{N+1}$ are small: $\nu, d \ll 1$ for $\beta = D = 1$ and large system size $N \gg 1$.

First, we find the linear modes of the disordered system ($d \neq 0$, $\nu = 0$) and analyze their properties. We compute the new eigenvectors $\hat{z}_{qn}$ defined through the transformation $x_n(t) = \sum_{q=1}^{N} Q_q(t)\hat{z}_{qn}$. We apply a perturbational approach for the harmonic mode q_0 using the small disorder parameter d: $Q_q(t) = Q_q^{(0)}(t) + dQ_q^{(1)}(t) + \ldots$, where $Q_q^{(0)}(t) = 0$ for $q \neq q_0$. In first order we obtain from eq. (2) the equation of a forced oscillator for modes with $q \neq q_0$: $\ddot{Q}_q^{(1)} + \omega_q^2 Q_q^{(1)} = -\omega_q \omega_{q_0} K_{q,q_0} Q_{q_0}^{(0)}$. As a result we find for the amplitude A of each mode

$$A_{q,q_0}^{(1)} = -\frac{\omega_q \omega_{q_0}}{\omega_q^2 - \omega_{q_0}^2} K_{q,q_0} A_{q_0}, \; q \neq q_0. \quad (3)$$

For eq. (3) being valid we request that the time-averaged mode energies satisfy $\langle E_{q_0+1} \rangle \ll E_{q_0}$, which translates into the condition

$$q_0 \ll q_c = 2\sqrt{2}(N+1)^{1/2}/D\sigma_\kappa. \quad (4)$$

Note that this condition coincides with the existence criterion for q-breathers [13].

It follows that normal modes with mode numbers $q_0 \ll q_c$ approximately keep their plane-wave eigenvector profile

$$\hat{z}_{q_0 n} = \sqrt{\frac{2}{N+1}} \times \left(\sin\frac{\pi q_0 n}{N+1} - d\sum_{p\neq q_0} \frac{\omega_{q_0}\omega_p}{\omega_{q_0}^2 - \omega_p^2} K_{q_0,p} \sin\frac{\pi p n}{N+1}\right) \quad (5)$$

in real space in the presence of disorder. Therefore these *metallic* modes are still delocalized in real space. On the other side, disorder leads to Anderson localization and implies that the eigenmodes of a one-dimensional disordered chain are localized. Therefore q_c sets a mobility edge: for $q_0 \ll q_c$ the *metallic* eigenmodes are delocalized in real space, and for $q_0 > q_c$ the *insulating* eigenmodes are localized. Note, that for finite length chains and for weak disorder *all modes* are metallic and delocalized if $q_c \geqslant N$. With eq. (4) such a complete delocalization in real space takes place for $N \leqslant 8/D^2\sigma_\kappa^2$. Note that a transfer matrix approach [8] yields a lower boundary q_c for spatially localized eigenstates which satisfies the same scaling $q_c \propto N^{1/2}$. Therefore a disordered harmonic chain contains a thin layer of $\sqrt{N}$ metallic modes with frequencies $0 \leqslant \omega \leqslant \omega_c \sim N^{-1/2}$. The eigenvectors of these modes are close to the eigenvectors of the unperturbed modes of the ordered harmonic chain.

Let us add anharmonic terms, and compute the periodic orbits which correspond to a continuation of the metallic modes of the disordered harmonic chain. These periodic orbits are coined q-breathers [12]. We introduce $\{\hat{Q}_q, \hat{P}_q\}$ such that $x_n(t) = \sum_{q=1}^{N} \hat{Q}_q(t)\hat{z}_{qn}$. It follows that

$$\ddot{\hat{Q}}_q + \omega_q^2 \hat{Q}_q = -\frac{\nu}{2}\sum_{p,r,s=1}^{N} C_{q,p,r,s}\omega_q\omega_p\omega_r\omega_s \hat{Q}_p\hat{Q}_r\hat{Q}_s + \frac{\nu d}{2}\sum_{p,r,s=1}^{N} \omega_q\omega_p\omega_r\omega_s \hat{Q}_p\hat{Q}_r\hat{Q}_s \left(\sum_{u\neq q} C_{t,p,r,s}\frac{\omega_u^2}{\omega_u^2 - \omega_q^2} K_{u,q} + 3\sum_{u\neq p} C_{q,u,r,s}\frac{\omega_u^2}{\omega_u^2 - \omega_p^2} K_{u,p}\right) + \text{h.o.t.} \quad (6)$$

We perform a perturbation expansion using the small parameter ν. We take $\hat{z}_{q_0 n}$ as the zeroth-order solution. Neglecting the higher-order terms $\mathcal{O}(\nu d)$, we obtain a q-breather state [12], whose energy distribution is exponentially localized in the metallic-mode space part:

$$E_{(2n+1)q_0} = \lambda^{2n} E_{q_0}\ ,\ \lambda = \frac{3\beta E_{q_0}(N+1)}{8\pi^2 q_0^2}. \qquad (7)$$

For $\lambda < 1$ the amplitudes of insulating modes are exponentially small and can be neglected.

Extensive calculations yield that $\mathcal{O}(\nu d)$ terms in the equations of motion lead to order $\mathcal{O}(\nu^2 d^2)$ energies of the high-frequency modes $q \gg q_0$:

$$\frac{\langle E_q \rangle}{E_{q_0}} \approx 63\nu^2 d^2 \sigma_\kappa^2, \qquad (8)$$

and can be neglected in the limit $N \to \infty$.

We conclude that disordered linear metallic modes with $q_0 \ll q_c$ continue into the nonlinear regime as q-breathers exponentially localized in the metallic-mode space part.

High energies lead to delocalization of metallic modes in the mode space, strong chaos, and nonlinearity-driven conductivity. In this case one cannot neglect nonlinear interaction between q-breathers and must consider the whole layer of metallic modes. To determine the strong stochasticity threshold we construct s-dimensional q-tori [14] by continuing the $s \ll q_c$ lowest-frequency metallic modes into the nonlinear regime. For small energies these objects are exponentially localized in the metallic-mode space part:

$$E_p/E_0 \propto (\lambda_T)^{2p}, \qquad \lambda_T = \beta N E_0/s, \qquad (9)$$

where E_0 and E_p are the average energies of the modes $\overline{1,s}$ and $\overline{(2p-1)s+1,(2p+1)s}$ [14]. Delocalization of tori happens when $\lambda_T > 1$. With $s \propto q_c$ the strong stochasticity threshold reads

$$N_{sst} \propto 1/D^2 \sigma_\kappa^2 \beta^2 E_0^2. \qquad (10)$$

Below the strong stochasticity threshold we expect three basic heat conductivity channels (fig. 1). (I) Metallic modes carry the heat flux ballistically by direct interaction with the heat baths, as in the linear case. The interaction strength, and therefore the mode-specific heat flux, are proportional to the squared amplitudes of the metallic eigenvectors next to the boundaries $j_q \propto \hat{z}^2_{q,n=1,N}$ [7]. For fixed boundary conditions $j = \sum_{q<q_c} j_q \propto N^{-3/2}$ and $\mathcal{K} \propto N^{-1/2}$. Therefore, the boundary resistance between the heat bath and the metallic modes grows with increasing system size. (II) Insulating localized Anderson modes interact with each other due to anharmonicity, and are opening a diffusive energy transport channel with a heat conductivity $\mathcal{K}(T)$ being independent of the system size N [15,16]. (III) Anharmonicity also opens a third conductivity channel, by reducing the boundary resistance for

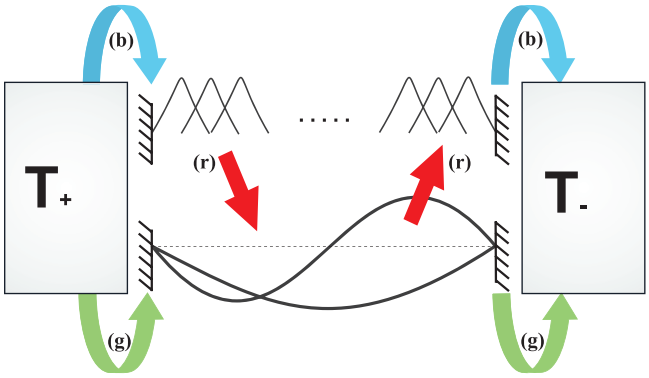

Fig. 1: (Color online) Schematic representation of conductance channels. Thick black metallic modes and thin black insulating modes are shown. Blue (b) and green (g) arrows show the energy fed into insulating and metallic modes channels by direct interaction with the heat baths. Nonlinearity also induces a heat flux from the insulating modes into the metallic ones and back (red (r) arrows).

metallic modes. This happens due to the thermalization among the insulating modes. Heat is then flowing from the insulating modes into the metallic modes, carried by the metallic modes through the system, and ejected again via an interaction with the insulating modes at the other end of the system. This third channel therefore eliminates the otherwise growing boundary resistance due to fixed boundary conditions.

The first conductivity channel (I) will be dominant when the average temperature T is low and the system length N is short enough. Increasing the system size leads to an increase in the boundary resistance and a reduction of the heat conductivity. The heat current via the second localized mode channel (II) can be estimated using recent studies of wave packet evolutions in disordered Klein-Gordon chains [17] and related heat conductivity studies [16]. For a given energy density (respectively, finite temperature) the diffusion rate (and therefore also the heat conductivity) are predicted to vary as $\mathcal{K} \sim T^2$ for $T > T_{cr}$ and $\mathcal{K} \sim T^4$ for $T < T_{cr}$. Here the crossover temperature T_{cr} is a model-dependent temperature which depends on the strength of disorder. Note that this heat conductivity value does not depend on the size of the system. Therefore the second channel will dominate over the first one if $N > N_{12}(T)$ where $N_{12}(T)$ is some function which increases with decreasing temperature. The crossover to normal conductivity will be observed at $N \approx N_{12}(T)$.

The heat conductivity through the third conductivity channel is obtained by realizing that the transfer of heat from insulating modes into metallic modes does not depend on the system size, but only on the temperature. It effectively replaces the fixed boundaries by open ones as concerning the metallic modes, and leads to a heat conductivity $\mathcal{K} \propto N^{1/2}$. Thus, for $N > N_{23}(T)$ we expect to observe a crossover from normal conductivity to anomalous $\alpha \approx 0.5$. Finally, with further increasing of

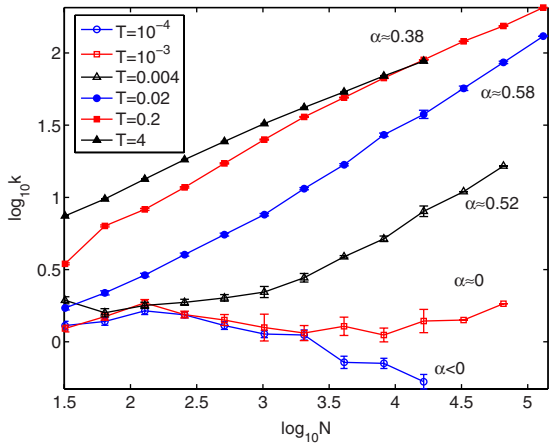

Fig. 2: (Color online) The averaged heat conductivity *vs.* chain length for different mean temperatures and $\beta = D = 1$. The values of the estimated exponents α are shown as well. Error bars quantify the statistical fluctuations.

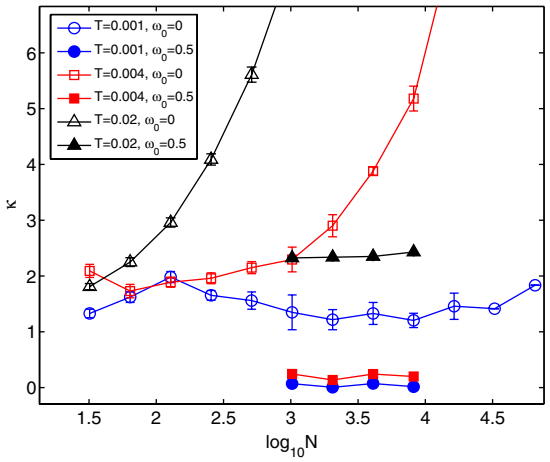

Fig. 3: (Color online) The averaged heat conductivity *vs.* chain length with (open symbols) and without (filled symbols) additional random on-site harmonic potentials for different mean temperatures and $\beta = D = 1$.

the system size N, the strong stochasticity threshold (10), $E_0 \equiv T$, is reached for $N > N_{sst}$. Then metallic modes start to strongly interact with each other, and theoretical predictions of fully developed turbulence within renormalization group approaches and mode coupling theories [9] become applicable and yield $\alpha \sim 1/3, \ldots, 2/5$.

To summarize, we expect that heat is carried by: i) ballistic metallic modes directly coupled to the heat reservoirs for $N < N_{12}$ with $\alpha \approx -1/2$; ii) insulating localized modes interacting with each other for $N_{12} < N < N_{23}$ with $\alpha \approx 0$; iii) ballistic metallic modes which are coupled to the heat reservoir via insulating localized modes for $N_{23} < N < N_{sst}$ with $\alpha \approx 1/2$; iv) strongly interacting metallic modes which are coupled to the heat reservoir via insulating localized modes for $N_{sst} < N$ with $\alpha \approx 1/3, \ldots, 2/5$.

We performed numerical simulations with integration time varying from 10^6 for the shortest chains to $2 \cdot 10^7$ for the longest, and with up to 100 disorder realizations. In all simulations $\beta = D = 1$. The observation of the predicted regimes at a single given temperature was not possible, since the needed chain sizes and corresponding integration times exceeded the limits set by our computational equipment. Therefore we use the temperature as an additional parameter, which shifts critical system sizes separating different regimes to lower values, as temperature increases. At $T = 10^{-4}$ we observe the first conductivity channel I with $\alpha < 0$ (fig. 2). Heat is transported by the metallic modes, and the increasing boundary resistance of the contact between them and the heat bath is responsible for the decrease of the conductivity with increasing system size. For the larger temperature $T = 0.001$ the second conductivity channel II starts to dominate. It leads to a conductivity which practically does not depend on the system size in the computationally available window. Here the heat flows predominantly through the insulating modes which are interacting with each other due to the anharmonicity of the interaction potential. At the even larger temperature $T = 0.004$ we observe the crossover to the conductivity channel III with the exponent $\alpha \approx 0.52$ for large N, with even slightly larger α at higher temperatures. Now the heat flows from the heat bath into the insulating modes at the boundaries, and is then transferred into the metallic modes. This leads to an effective decrease of the contact resistance between the metallic modes and the heat bath. The metallic modes then transport the heat ballistically through the chain, and eject it in the same manner at the opposite end of the chain. To confirm that in this regime indeed the metallic modes are transporting the heat through the chain, we add a random on-site harmonic potential $\frac{1}{2}\sum_{n=1}^{N} \Omega_n^2 x_n^2$, $\Omega_n \in [0; \omega_0]$ to (1). This opens a gap in the frequency spectrum of the harmonic chain at low frequencies. Therefore the total momentum is not anymore conserved, the mobility edge is vanishing, and metallic modes turn into insulating modes as well. Then the third channel III ceases to exist, and heat should be again transported via channel II. As a result we expect that the heat conductivity becomes independent of the system size. Indeed, our numerical results confirm this prediction (fig. 3).

At the largest studied temperatures, we observe the fourth conductivity channel IV with exponent $\alpha \approx 0.38$ ($T = 0.2$ and $T = 4$, fig. 2). At variance to the regime III, the metallic modes are now strongly interacting with each other while transporting the heat through the chain.

In conclusion, we shed light on the complex interplay between disorder and nonlinearity that determines the heat conductivity of anharmonic acoustic chains, revealing a much more intricate picture than expected before. We predict and observe four different heat flow channels: i) ballistic transfer by metallic delocalized modes coupled directly to the heat baths, ii) diffusive transfer by the insulating localized modes, iii) ballistic transfer by

metallic delocalized modes, coupled to the heat baths via the insulating localized modes, iv) turbulent transfer by metallic delocalized modes due to strong mode-mode interaction. The corresponding size dependence of the conductivity coefficient is drastically different: insulating, normal, and two types of anomalous dependence. The studied system sizes are comparable to the number of atoms along nanotubes; therefore, the predicted crossovers may prove to be observable even in the current experimental systems, if the temperature is varied.

* * *

Computations were carried out at the HPC University of Nizhniy Novgorod and MPIPKS. The support of Prof. V. P. Gergel is appreciated. MVI acknowledges the support of Dynasty Foundation, the Federal Program "Scientific and scientific-diductional brainpower of innovative Russia" for 2009–2013 (contracts П2308, 02.740.11.0839) and RFBR 10-02-00865 We thank G. Casati, S. Lepri, R. Schilling, S. Aubry and N. Li for helpful discussions.

REFERENCES

[1] Chang C. W. *et al.*, *Science*, **314** (2006) 1121; Chang C. W. *et al.*, *Phys. Rev. Lett.*, **99** (2007) 045901.
[2] Chang C. W. *et al.*, *Phys. Rev. Lett.*, **101** (2008) 075903.
[3] Schwab K. *et al.*, *Nature*, **404** (2000) 974; Yang N., Zhang G. and Li B., *Nano Today*, **5** (2010) 85.
[4] Stoltz G., Lazzeri M. and Mauri F., *J. Phys.: Condens. Matter*, **21** (2009) 245302.
[5] Savin A. V., Hu B. and Kivshar Y. S., *Phys. Rev. B*, **80** (2009) 195423.
[6] Payton D. N., Rich M. and Visscher W. M., *Phys. Rev.*, **160** (1967) 706; Jackson E. A., Pasta J. R. and Waters J. F., *J. Comput. Phys.*, **2** (1968) 207; Ishii K., *Suppl. Prog. Theor. Phys.*, **53** (1973) 77; Prosen T. and Campbell D. K., *Phys. Rev. Lett.*, **84** (2000) 2857.
[7] Lepri S., Livi R. and Politi A., *Phys. Rep.*, **377** (2003) 1; Dhar A., *Adv. Phys.*, **57** (2008) 457.
[8] Matsuda H. and Ishii K., *Suppl. Prog. Theor. Phys.*, **45** (1970) 56.
[9] Narayan O. and Ramaswamy S., *Phys. Rev. Lett.*, **89** (2002) 200601; Lepri S., *Phys. Rev. E*, **58** (1998) 7165; Dhar A., *Phys. Rev. Lett.*, **86** (2001) 3554; Casati G. and Prosen T., *Phys. Rev. E*, **67** (2003) 015203; Lee-Dadswell G. R., Nickel B. G. and Gray C. G., *Phys. Rev. E*, **72** (2005) 031202.
[10] Li B., Zhao H. and Hu B., *Phys. Rev. Lett.*, **86** (2001) 63.
[11] Dhar A. and Saito K., *Phys. Rev. E*, **78** (2008) 061136.
[12] Flach S., Ivanchenko M. V. and Kanakov O. I., *Phys. Rev. Lett.*, **95** (2005) 064102; *Phys. Rev. E*, **73** (2006) 036618.
[13] Ivanchenko M. V., *Phys. Rev. Lett.*, **102** (2009) 175507.
[14] Christodoulidi H., Efthymiopoulos C. and Bountis T., *Phys. Rev. E*, **81** (2010) 016210.
[15] Casati G. *et al.*, *Phys. Rev. Lett.*, **52** (1984) 1861; Hu B., Li B. and Zhao H., *Phys. Rev. E*, **61** (2000) 3828.
[16] Flach S., Ivanchenko M. V. and Li N., to be published in *Pramana - J. Phys.*, arXiv:1101.4530 (2011).
[17] Flach S. *et al.*, *Phys. Rev. Lett.*, **102** (2009) 024101; Skokos Ch. *et al.*, *Phys. Rev. E*, **79** (2009) 056211; Skokos Ch. *et al.*, *Phys. Rev. E*, **82** (2010) 016208; Lapteva T. V. *et al.*, *EPL*, **91** (2010) 30001.